

2933

Inaccurate Visualisation of Haemorrhagic Markers in Cerebral Amyloid Angiopathy in Susceptibility Weighted Imaging can be Overcome Using Susceptibility Mapping

Barbara Dymerska¹, Gargi Banerjee², Emma Dixon¹, Emma Biondetti¹, Anna Barnes³, Jonathan Schott⁴, Nick Fox⁴, Rolf Jager⁵, Karin Shmueli¹, David Werring², and David L. Thomas^{2,6}

¹Department of Medical Physics and Biomedical Engineering, University College London, London, United Kingdom, ²Department of Brain Repair and Rehabilitation, UCL Queen Square Institute of Neurology, University College London, London, United Kingdom, ³Institute of Nuclear Medicine, University College London, London, United Kingdom, ⁴Dementia Research Centre, UCL Queen Square Institute of Neurology, University College London, London, United Kingdom, ⁵Lysholm Department of Neuroradiology and the Neuroradiological Academic Unit, UCL Queen Square Institute of Neurology, University College London, London, United Kingdom, ⁶Leonard Wolfson Experimental Neurology Centre, UCL Queen Square Institute of Neurology, University College London, London, United Kingdom

Synopsis

Cerebral amyloid angiopathy is a small vessel disease characterised by imaging signatures including cerebral microbleeds and cortical superficial siderosis. We show here that non-local phase effects affecting Susceptibility Weighted Imaging (SWI) cause broadening and/or duplication of microbleeds, as well as deformation of superficial siderosis. Furthermore, susceptibility maps and “true SWI”, where local susceptibility values are used, facilitate more accurate microbleed size estimation, reduce the risk of microbleed miscount and provide better delineation of superficial siderosis. Therefore, susceptibility maps and true SWI are likely to be more accurate than SWI in identifying and grading these haemorrhagic markers, with potential clinical relevance.

Introduction

Cerebral Amyloid Angiopathy (CAA) is a small vessel disease characterised by the agglomeration of amyloid mostly in the cortical and leptomeningeal arteries and arterioles⁽¹⁾. Its prevalence reaches 20–40% in non-demented and 50–60% in demented elderly populations^(2,3). Whilst no definite CAA identification can be made without histopathology, CAA can be diagnosed in vivo using MRI-detectable markers including IntraCerebral Haemorrhage (ICH), Cerebral MicroBleeds (CMB), and cortical Superficial Siderosis (cSS)^(4–7). A recently developed CAA score attempts to estimate disease severity using measures including the number of CMBs and sulci affected by cSS⁽⁸⁾. Accurate quantification of these markers is thus essential for diagnosis and patient management in CAA and other cerebral small vessel diseases⁽⁹⁾. Here, we show improved identification of CMB and cSS by replacing non-local MRI phase with underlying local susceptibility values in Susceptibility Weighted Imaging (SWI)⁽¹⁰⁾.

Methods

Data were collected as part of the BOCAA (Biomarkers and Outcomes in Cerebral Amyloid Angiopathy) study, approved by the local ethics committee. Ten patients with “probable CAA”, according to the Boston criteria⁽⁴⁾ (age: 68.6±3.0 years, 2 women) and five healthy volunteers (age: 64.4±6.5 years, 3 women) were scanned on a 3 T Siemens Magnetom Biograph mMR using a 12-channel head coil and a 3D GRE sequence⁽¹¹⁾: TEs = [4.9, 9.8, 19.7] ms, TR = 27 ms, Receiver Bandwidth = [400, 400, 140] Hz/Pixel, Flip Angle = 15°, Matrix Size = 192x256x96 voxel³, Resolution = 0.9x0.9x1.5 mm³. The phase and magnitude images were combined using ASPIRE⁽¹²⁾. Laplacian unwrapping was applied to the combined phase at TE = 19.7 ms. The unwrapped phase was High-Pass Filtered (HPF) using a 5x5x3 voxel Gaussian kernel with standard deviation of 2 voxels. Additionally, instead of HPF, background fields were removed with PDF⁽¹³⁾ and susceptibility maps (SM) were calculated using Tikhonov regularisation with regularisation parameter = 0.05⁽¹⁴⁾. Phase and SM masks were created, where values were set to “1” for negative phase or susceptibility, and decreased linearly to “0” for values between zero and the maximum. Masks were raised to the power of 4 and multiplied by the corresponding magnitude image yielding classical SWI⁽¹⁵⁾, with the phase mask, and “true SWI” (tSWI)⁽¹⁰⁾, using SM mask.

Results

All CAA patient images showed CMBs and/or cSS whereas healthy control images showed no such pathology.

Figures 1 and 2 show examples of artifactual CMB duplication or broadening in SWI in two patients with a light and a heavy CMB burden respectively. In Figure 1A the arrow shows a CMB clearly visible in the HPF phase and SWI but not in the magnitude image, SM and tSWI. The sagittal view of the same CMB (Fig. 1B, arrow) reveals a dipole-like field distribution in the HPF phase surrounding the CMB. This creates two hypointense spots along the B₀ direction in the phase mask, causing artifactual CMB broadening in SWI, which could be misinterpreted as two neighbouring CMBs. Both the SM and corresponding tSWI are free of this non-local artifact, revealing a single focal susceptibility increase at the CMB. In Figure 2A four apparent CMBs are marked in the SWI, which are not visible in the corresponding magnitude image, SM and tSWI.

Figure 3 shows a patient with disseminated cSS where cortical surfaces appear artifactually deformed in the SWI (Fig. 3A, arrow). The cSS layer is shown clearly in the SM (bright) and tSWI (dark). Non-local phase effects are especially apparent in the sagittal view for cortical surfaces perpendicular to the main magnetic field (Fig. 3B, arrow).

Figure 4 shows two axial slices from a patient whose entire cortical surface appears hypointense in SWI and could therefore be interpreted as disseminated cSS. These hypointensities are less apparent in tSWI, suggesting that the cSS may not be as extensive as the SWI indicates.

All SMs and tSWI were characterised by superior image quality and less noise compared to SWI.

Discussion and conclusions

We have shown that non-local phase effects in SWI cause broadening and/or duplication of CMBs and deformation of cSS, which may lead to CMB miscount and misestimation of cSS extent respectively. SM and tSWI provided better image quality than SWI, facilitating more accurate CMB size estimation and cSS delineation, and reducing the risk of CMB miscount. By using the underlying susceptibility instead of non-local phase values, SM and

tSWI are likely to be more accurate than SWI in identifying and grading haemorrhagic markers of CAA which are essential for diagnosis and estimating disease severity. Therefore, SM and tSWI may aid clinical management of patients with CAA and other haemorrhagic cerebral small vessel diseases.

Acknowledgements

The BOCAA study is funded by Rosetrees Trust Fund. BD is supported by Marie Skłodowska-Curie Action (MRI COMIQUISUM #798119) and DLT by the UCL Leonard Wolfson Experimental Neurology Centre (PR/ylr/18575).

References

- Biffi A, Greenberg SM. Cerebral Amyloid Angiopathy: A Systematic Review. *Journal of Clinical Neurology* 2011;7:1 doi: 10.3988/jcn.2011.7.1.1.
- Xuereb JH, Brayne C, Dufouil C, et al. Neuropathological Findings in the Very Old: Results from the First 101 Brains of a Population-based Longitudinal Study of Dementing Disorders. *Annals of the New York Academy of Sciences* 2000;903:490–496 doi: 10.1111/j.1749-6632.2000.tb06404.x.
- Charidimou A, Gang Q, Werring DJ. Sporadic cerebral amyloid angiopathy revisited: recent insights into pathophysiology and clinical spectrum. *J Neurol Neurosurg Psychiatry* 2012;83:124–137 doi: 10.1136/jnnp-2011-301308.
- Knudsen KA, Rosand J, Karluk D, Greenberg SM. Clinical diagnosis of cerebral amyloid angiopathy: validation of the Boston criteria. *Neurology* 2001;56:537–539.
- Linn J, Halpin A, Demaerel P, et al. Prevalence of superficial siderosis in patients with cerebral amyloid angiopathy. *Neurology* 2010;74:1346–1350 doi: 10.1212/WNL.0b013e3181dad605.
- Banerjee G, Carare R, Cordonnier C, et al. The increasing impact of cerebral amyloid angiopathy: essential new insights for clinical practice. *J Neurol Neurosurg Psychiatry* 2017;jnnp-2016-314697 doi: 10.1136/jnnp-2016-314697.
- Dierksen GA, Skehan ME, Khan MA, et al. Spatial relation between microbleeds and amyloid deposits in amyloid angiopathy. *Annals of Neurology* 2010;68:545–548 doi: 10.1002/ana.22099.
- Charidimou A, Martinez-Ramirez S, Reijmer YD, et al. Total Magnetic Resonance Imaging Burden of Small Vessel Disease in Cerebral Amyloid Angiopathy: An Imaging-Pathologic Study of Concept Validation. *JAMA Neurol* 2016;73:994–1001 doi: 10.1001/jamaneurol.2016.0832.
- Haller S, Vernooij MW, Kuijper JPA, Larsson E-M, Jäger HR, Barkhof F. Cerebral Microbleeds: Imaging and Clinical Significance. *Radiology* 2018;287:11–28 doi: 10.1148/radiol.2018170803.
- Liu S, Mok K, Neelavalli J, et al. Improved MR venography using quantitative susceptibility-weighted imaging. *Journal of Magnetic Resonance Imaging* 2014;40:698–708 doi: 10.1002/jmri.24413.
- Lane CA, Parker TD, Cash DM, et al. Study protocol: Insight 46 – a neuroscience sub-study of the MRC National Survey of Health and Development. *BMC Neurology* 2017;17:75 doi: 10.1186/s12883-017-0846-x.
- Eckstein K, Dymerska B, Bachrata B, et al. Computationally Efficient Combination of Multi-channel Phase Data From Multi-echo Acquisitions (ASPIRE). *Magnetic Resonance in Medicine* 2018;79:2996–3006 doi: 10.1002/mrm.26963.
- Liu T, Khalidov I, Rochefort L de, et al. A novel background field removal method for MRI using projection onto dipole fields (PDF). *NMR in Biomedicine* 2011;24:1129–1136 doi: 10.1002/nbm.1670.
- Kressler B, de Rochefort L, Liu T, Spincemaille P, Jiang Q, Wang Y. Nonlinear Regularization for Per Voxel Estimation of Magnetic Susceptibility Distributions from MRI Field Maps. *IEEE Trans Med Imaging* 2010;29:273–281 doi: 10.1109/TMI.2009.2023787.
- Haacke EM, Xu Y, Cheng Y-CN, Reichenbach JR. Susceptibility weighted imaging (SWI). *Magnetic Resonance in Medicine* 2004;52:612–618 doi: 10.1002/mrm.20198.

Figures

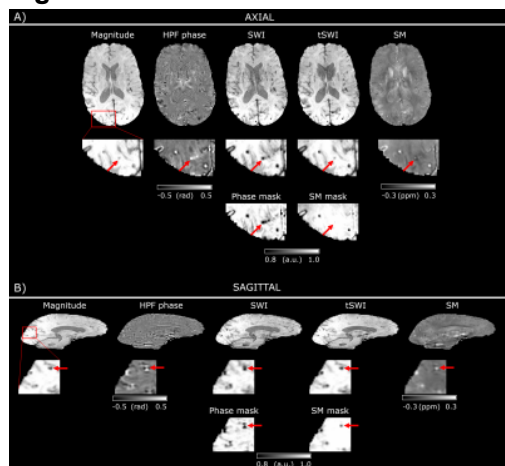


Fig.1 An example of CMB broadening/duplication in a CAA patient with a light CMB burden. Arrows mark the same pathology, which is apparent in a selected axial slice (A) in the HPF phase and SWI but not in the magnitude image, susceptibility map (SM) and corresponding true SWI (tSWI). This effect can be clearly explained by looking at the dipole-like distribution of the HPF phase in sagittal view (B), which appears as two hypointensities in the phase

mask and causes the broadening/duplication of CMB in SWI. In the SM and corresponding tSWI this CMB preserves its small spherical shape.

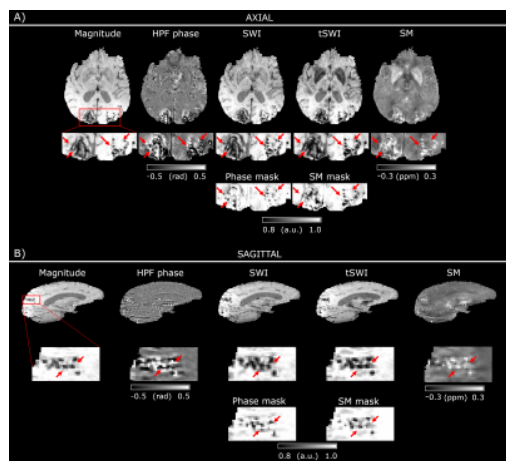


Fig.2 An example of CMB broadening and/or duplication in a CAA patient with a heavy CMB burden and a lobar ICH. A) the arrows show four CMBs apparent in the HPF phase and SWI but not in the magnitude, SM and tSWI. As in Fig. 1, this effect can be explained by looking at B) where the dipole-like distributions of the HPF phase around CMBs appear as two hypointensities per CMB in the phase mask and causes the broadening or duplication of CMB in SWI. In the SM and the corresponding tSWI the CMBs preserve their small spherical shapes.

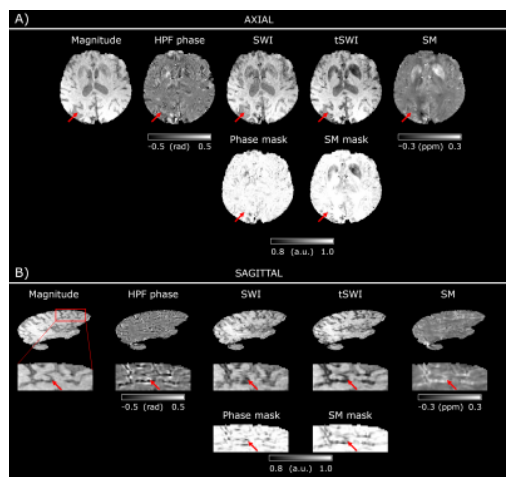


Fig.3 An example of artifactual deformation of cSS in SWI caused by the non-local phase distribution (see arrow). The susceptibility map and tSWI show much clearer delineation of cSS in both, axial (A) and sagittal (B) views.

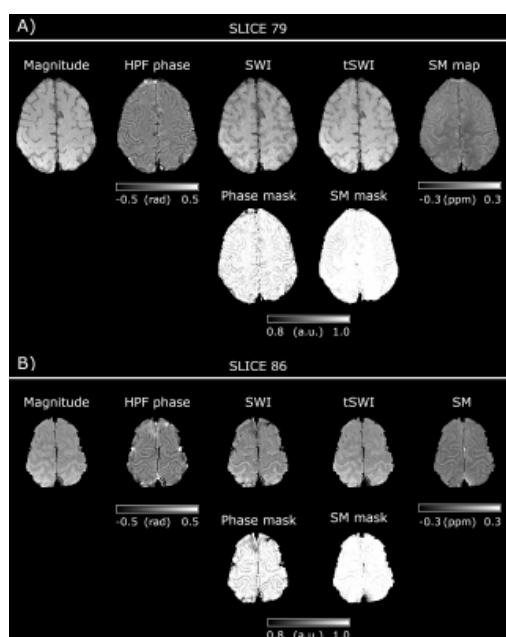


Fig.4 Two axial slices from a patient with hypointensities along the entire cortical surface in the HPF phase and SWI which may be interpreted as disseminated cSS. These hypointensities are less apparent in the SM and tSWI, suggesting that cSS may not be as extensive as it appears in the SWI.

